BUILDING FOOTPRINTS EXTRACTION OF DENSE RESIDENTIAL AREAS FROM LIDAR DATA

KyoHyouk Kim and **Jie Shan**
Purdue University
School of Civil Engineering
550 Stadium Mall Drive
West Lafayette, IN 47907, USA
{kim458, jshan}@purdue.edu

ABSTRACT

Extracting individual buildings and determining their footprints have been extensively studied towards 3D Building reconstruction. Though most previous works show promising results, it is yet a nontrivial task, especially in dense residential areas. This paper discusses a methodology for resolving this issue. The proposed approach starts with separating ground and nonground LiDAR points. In the subsequent step, non-planar points lying on the discontinuity are removed by analyzing the consistency of the normal vectors. The remaining planar points are clustered into a set of individual building blobs. Finally, building footprint for each building is determined by applying alpha-shape and polyline simplification algorithm.

KEYWORDS: LiDAR (Light Detection And Ranging), Segmentation, Building boundary extraction, Haiti, Classification

INTRODUCTION

3D building reconstruction has been one of the most active research topics in remote sensing community due to its various applications. Extracting individual buildings is a critical step toward automatic 3D building reconstruction. Various data sources such as LiDAR point clouds (Neidhart and Sester 2008), digital surface model (Tournaire, Breif et al.) and high resolution satellite imagery (Awrangjeb, Ravanbakhsh et al.) have been used for this purpose. Though previous approaches work quite well, it is still ongoing research topic to get better results, especially in the complex landscapes or dense residential areas. There are fundamental differences among different data sources, which affect the quality of the final results. While digital surface model enables one to apply certain algorithms with a straightforward data structure, it often misses details of the original point clouds. In contrast, the direct manipulation of LiDAR points generally requires more intensive computation and larger amount of data storage. Furthermore, it often suffers from noisy measurements.

Building footprints extraction is commonly approached by a few successive steps, i.e. (1) separating ground and nonground points, (2) isolating individual buildings, (3) determining building footprints and (4) generalizing boundary line segments. The main objective of the first step is to differentiate nonground points from ground points. This can be accomplished by a number of filtering algorithms, such as morphological filtering (Zhang, Chen et al. 2003; Arefi and Hahn 2005), adaptive TIN densification (Axelsson 2000) or labeling process (Shan and Sampath 2005). In the subsequent step, nonground points are further processed to extract only building points. The first and last returns (Alharthy and Bethel 2002) or eigenvalue analysis of local covariance matrix (Verma, Kumar et al. 2006; Sampath and Shan 2010) can be used for this process. For the 3rd and 4th tasks above, building boundary points are first determined. Alpha-shape (Edelsbrunner, Kirkpatrick et al. 1983) or modified convex-hull (Sampath and Shan 2004) algorithm is commonly involved for this purpose. Finally, simplified footprints are determined by least square (Sampath and Shan 2004), RANSAC or Douglas-Peuker algorithm (Neidhart and Sester 2008).

This paper proposes a methodology for extracting building footprints, especially in a dense residential area. The main premise is that closely crowded buildings can be separated by discontinuities, in which normal vectors are not consistent. To evaluate this approach, extracted building footprints from the test area in Haiti are presented. Another result from object-based image classification is also presented for comparison.

FOOTPRINTS EXTRACTION

In the first step, nonground points are differentiated from ground points. We applied the similar approach as morphology based filtering algorithm (Zhang, Chen et al. 2003; Chen, Gong et al. 2007). The main difference is that morphological erosion operation is applied only to potential points lying on discontinuity. Various measures such as slope change or height difference can be used to identify these points. The algorithm begins with generating a regular grid with a predefined grid size, which is determined from either a fixed resolution or the average point density. Elevation of each cell is then assigned with that of LiDAR point falling in the cell. If more than one point falls in the same cell, the lowest elevation is selected, while the others are excluded. For an empty cell, the elevation of the closest LiDAR point is assigned. As in (Zhang, Chen et al. 2003), each cell keeps the index of the original LiDAR points. Therefore, morphological filtering applied to the grid directly separates the original LiDAR point clouds. In the subsequent step, morphological erosion operation is applied to either row-wise or column-wise direction with three consecutive cells. As shown in Figure 1(a)-(d), trees or noisy points are eliminated within the first a few iterations, while building points with various sizes are eliminated in further iterations. In this research, the proposed filtering is applied to both direction, i.e. column and row-wise, and the union of two sets of nonground points are chosen as the final nonground points, while the other points are removed as ground points.

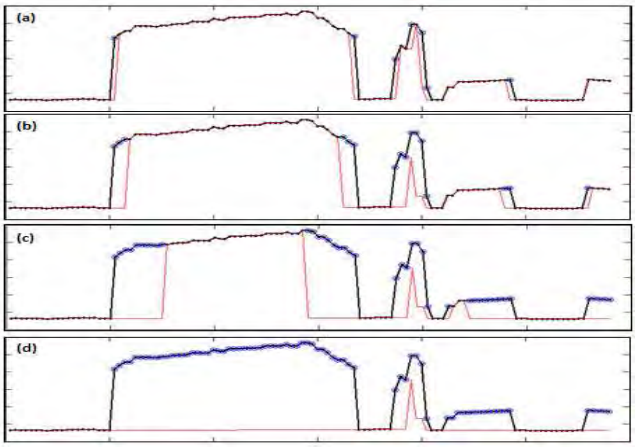

Figure 1. Filtering of a LiDAR profile, (a)-(d) Intermediate plots of different iteration steps, (black dots) lidar points, (blue dots) filtered nonground points and (red line) morphologically eroded surface.

Local Planarity

Once nonground and ground points are separated, local planarity of nonground points is analyzed. First, normal vectors of all nonground points are determined. To compute more accurate normal vectors, a certain distance threshold is involved. In this study, two times an average point distance is used as the threshold for determining normal vectors. Once normal vectors of all nonground points are determined, nonground points are further separated into two groups, i.e. planar and non-planar points. Planar points can be identified by several methods, such as PCA (Principal Component Analysis) or dimensionality analysis (Verma, Kumar et al. 2006; Sampath and Shan 2008). The principle is that if a set of points lie on the plane, only two mutually orthogonal basis vectors are required to represent those points. Eigenvalues of the covariance matrix constructed from a set of neighborhood points provide the relevant information. For example, if the smallest eigenvalue is much less than the other two values, those points are considered as planar points, otherwise, non-planar points. Another approach is to analyze the mean angle difference of normal vectors at the given point with those of neighboring TIN triangles. This value should be zero if the point lies on the perfect plane. However, due to the inherent noise of LiDAR points, certain angle threshold is required. In this paper, 10^{o} is used as an angle threshold. Any points beyond this threshold are considered non-planar points and excluded in the subsequent process. The identified non-planar points correspond to those mostly lying on trees, building boundaries or step edges as shown in Figure 2.

Determination of Building Boundary

To determine building footprints, the remaining points need to be clustered into individual buildings. This is accomplished by comparing the distance among all LiDAR points. Points within the pre-defined distance threshold are grouped into the same building, while the other points are labeled as different building. This process is performed until no new building is added. The result of this process is shown in Figure 3. For each identified building blob, its footprint (i.e. building boundary) is determined as follows. First, boundary points are determined by applying alpha-shape algorithm (Edelsbrunner, Kirkpatrick et al. 1983) and rearranged in a successive order (Figure 3(b)). These points are then used as inputs for the polyline simplification algorithm, i.e. Douglas-Peuker algorithm (Douglas and Peucker 1973). The simplification is performed recursively within the pre-defined threshold. Any points beyond this threshold remain reflection points. As shown in Figure 3(c), reflection points mostly correspond to building corner points. In the last step, all boundary points between two consecutive reflection points are fitted by RANSAC and intersection points between two consecutive line segments are selected as corner points constituting final building footprint. This workflow is illustrated in Figure 3.

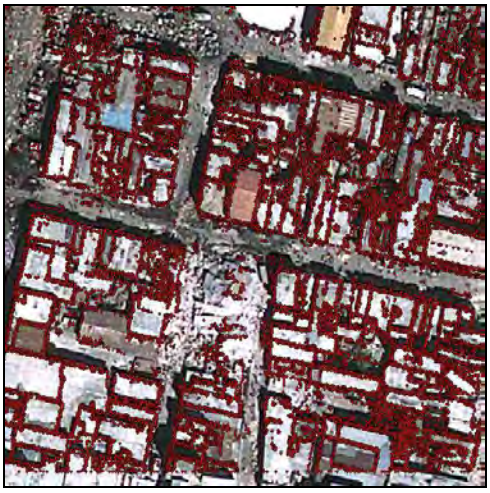

Figure 2. Identified non-planar points.

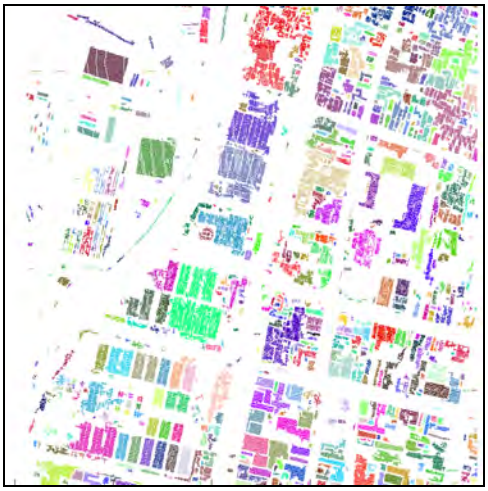

Figure 3. Separated individual building points.

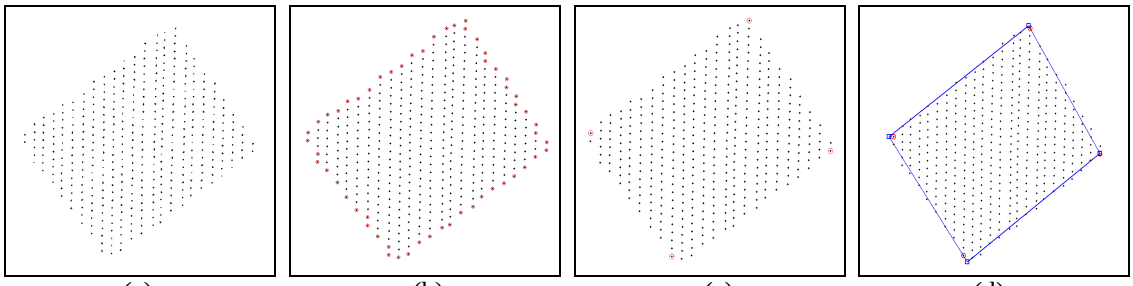

(a) (b) (c) (d)

Figure 4. Determination of building footprint, (a) building points; (b) building boundary points; (c) identified reflection points; (d) footprints (blue squares : building corner points).

INITIAL RESULTS AND CONCLUSIONS

The proposed approach is tested with LiDAR data around the Port-au-Prince in Haiti. This data is acquired with the help of Rochester Institute of Technology (RIT) as one of relief activities for the devastating earthquake occurred on January 12, 2010. Identifying building footprints can be used as valuable information for damage estimation or change detection caused by the earthquake. The problem is that most areas in Haiti show highly complex and heterogeneous patterns. Various types of buildings with different sizes are mixed up, which prevents us getting good results for identifying building footprints. The GeoEye-1 image of the test area and extracted footprints from the proposed approach are presented in Figure 5(a) and (b) respectively. Another result obtained from object-based image classification with GeoEye-1 image is also presented in Figure 5(c).

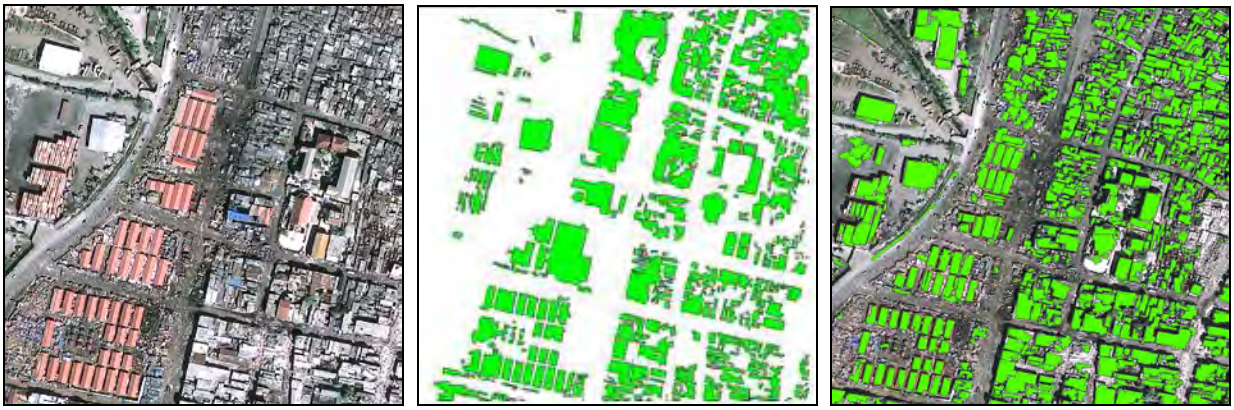

(a) (b) (c)

Figure 5. Initial result, (a) GeoEye-1 image; (b) result of the proposed approach; (c) result of object-based image classification with GeoEye-1 image.

In Figure 6, closer looks for two different areas are presented. It is seen that large and well-separated buildings are identified correctly in both results as shown in Figure 6(b) and (c). Our result (b) extract some smaller buildings (shown in the middle of Figure 6(a)), which are missed in the classification result (c). However, some of large buildings are connected to one building. This issue is mainly caused by rubble, debris or very small structures around buildings, which are not removed correctly. In the GeoEye-1 image shown in Figure 6(a), these buildings show distinctive spectral characteristic, such that better result can be easily obtained.

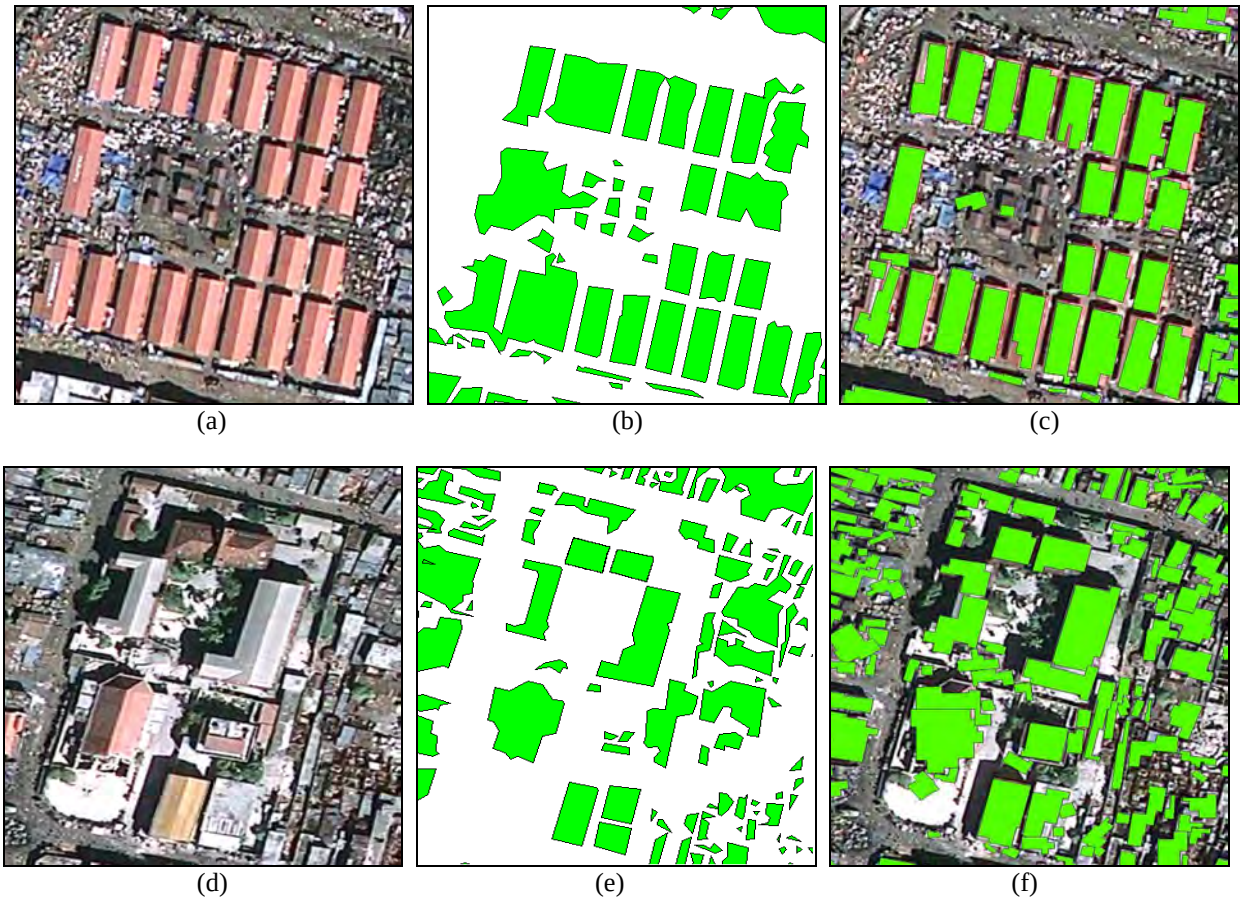

Figure 6. Comparison with image classification result, (a) and (d) GeoEye-1 images; (b) and (e) results of the proposed approach; (c) and (f) results of object-based image classification with GeoEye-1 image.

In Figure 6(d)-(f), another example is presented for a comparison. It is seen that some of large buildings (shown in the middle) are divided into separate pieces in the classification result (f), whereas our result produces correct building footprints as shown in Figure 6(b).

In this paper, we presented a methodology to extract building footprints from LiDAR point clouds. Once nonground points are differentiated from ground points, the consistency of normal vectors is analyzed to exclude non-planar points. In the subsequent step, the remaining planar points are clustered into a set of individual building blobs. Finally, building footprint for each building is determined. Though our initial experiments show promising results, some misconnected buildings are often identified. One of the reasons is that a few points are often remained within the distance between different buildings, which produces a misconnected larger building. This problem can be resolved through refining the filtering results.

REFERENCES

Alharthy, A. and J. Bethel (2002). "Heuristic filtering and 3D feature extraction from LiDAR data." International Archives of Photogrammetry, Remote Sensing and Spatial Information Sciences **34**(PART 3/A): 29-34.

Arefi, H. and M. Hahn (2005). A morphological reconstruction algorithm for separating off-terrain points from terrain points in laser scanning data. ISPRS Workshop "Laser scanning 2005", Enschede, the Netherlands.

Awrangjeb, M., M. Ravanbakhsh, et al. "Automatic detection of residential buildings using LIDAR data and multispectral imagery." ISPRS Journal of Photogrammetry and Remote Sensing.

Axelsson, P. (2000). "DEM generation from laser scanner data using adaptive TIN models." International Archives of Photogrammetry and Remote Sensing **33**(B4/1; PART 4): 111-118.

Chen, Q., P. Gong, et al. (2007). "Filtering airborne laser scanning data with morphological methods." Photogrammetric Engineering and Remote Sensing **73**(2): 175.

Douglas, D. and T. Peucker (1973). "Algorithms for the reduction of the number of points required to represent a digitized line or its caricature." Cartographica: The International Journal for Geographic Information and Geovisualization **10**(2): 112-122.

Edelsbrunner, H., D. Kirkpatrick, et al. (1983). "On the shape of a set of points in the plane." IEEE Transactions on Information Theory **29**(4): 551-559.

Neidhart, H. and M. Sester (2008). "Extraction of building ground plans from LiDAR data." International Archives of Photogrammetry, Remote Sensing and Spatial Information Sciences **37**(Part B2): 405-410.

Sampath, A. and J. Shan (2004). "Urban modeling based on segmentation and regularization of airborne lidar point clouds." International Archives of Photogrammetry, Remote Sensing and Spatial Information Sciences **35**: 937-942.

Sampath, A. and J. Shan (2008). "Building roof segmentation and reconstruction from LiDAR point clouds using clustering techniques." International Archives of Photogrammetry, Remote Sensing and Spatial Information Sciences **37**(PART B3a): 279-284.

Sampath, A. and J. Shan (2010). "Segmentation and reconstruction of polyhedral building roofs from aerial Lidar point clouds." IEEE Transactions on geoscience and remote sensing **48**(3): 1554-1567.

Shan, J. and A. Sampath (2005). "Urban DEM generation from raw lidar data: A labeling algorithm and its performance." Photogrammetric Engineering & Remote Sensing **71**(2): 217-226.

Tournaire, O., M. Breif, et al. "An efficient stochastic approach for building footprint extraction from digital elevation models." ISPRS Journal of Photogrammetry and Remote Sensing **65**(4): 317-327.

Verma, V., R. Kumar, et al. (2006). 3D Building detection and modeling from aerial LIDAR data. 2006 IEEE Computer Society Conference on Computer Vision and Pattern Recognition, CVPR'06. IEEE Computer Society, Washington, DC.

Zhang, K., S. C. Chen, et al. (2003). "A progressive morphological filter for removing nonground measurements from airborne LIDAR data." IEEE Transactions on Remote Sensing and Geoscience **41**(4): 872-882.